ARTICLES

Numerical investigation of two-dimensional pure electron plasma equilibria on magnetic surfaces

Thomas Sunn Pedersen
Department of Applied Physics and Applied Mathematics, Columbia University, New York, New York 10027

(Received 12 September 2002; accepted 21 October 2002)

Two-dimensional solutions to the equilibrium equation for finite temperature, low density pure electron plasmas confined on magnetic surfaces [T. S. Pedersen and A. H. Boozer, Phys. Rev. Lett. **88**, 205002 (2002)] are presented for the first time. These equilibria are not maximum energy states, in contrast to Penning trap equilibria [J. Notte *et al.*, Phys. Rev. Lett. **69**, 3056 (1992)]. By varying the number of Debye lengths in the plasma, a/λ_D, from 0.1 to 10, we explore both relatively warm and relatively cold plasma equilibria. The effects of different boundary conditions and the implications for collisional transport rates are discussed. © *2003 American Institute of Physics.* [DOI: 10.1063/1.1535208]

I. INTRODUCTION

This paper presents the first numerical study of equilibria of finite temperature pure electron plasmas confined on toroidal magnetic surfaces. Magnetic surface configurations, such as stellarators and tokamaks, are highly developed and studied in the context of thermonuclear fusion, and have recently become of interest for the confinement of non-neutral plasmas.[1,2] They have certain advantages over open and closed field line systems, such as the Penning trap,[3] which is the most successful configuration for confinement of single species plasmas. Magnetic surface configurations confine both positive and negative species simultaneously, at any level of charge imbalance from pure electron to quasineutral. They may provide stabilization of diocotron modes, and confine energetic electrons and positrons at modest magnetic field strengths. Thus, such configurations have unique advantages for laboratory confinement of positron–electron (pair) plasmas, non-neutral electron–ion plasmas, and antiproton–positron plasmas. The latter could facilitate creation of copious amounts of antihydrogen.

The finite temperature equilibrium for a pure electron plasma confined on magnetic surfaces is fundamentally different from those previously studied, implying that new physics is involved.[1] In this paper, we present the first numerical study of such equilibria in two dimensions. We show that the equilibrium equation can be derived by minimizing a suitably defined energy. The effects of different boundary conditions are explored in the two distinct physics regimes of the equilibrium, $a/\lambda_D \ll 1$ and $a/\lambda_D \gg 1$, where a is the characteristic (radial) size of the plasma and $\lambda_D = \sqrt{\epsilon_0 T_e/ne^2}$ is the Debye length. Implications for collisional transport time scales are discussed.

II. THEORY

The equilibrium equation for a finite-temperature, low-density pure-electron plasma in a magnetic surface configuration is[1]

$$\nabla^2\phi = \frac{e}{\epsilon_0} N(\psi)\exp\left(\frac{e\phi}{T_e(\psi)}\right). \tag{1}$$

Here, low density implies $n \ll n_B$, where $n_B = \epsilon_0 B^2/2m_e$ is the Brillouin density.[4] ψ is the magnetic surface coordinate, that is, the $\psi =$ constant surfaces are the magnetic surfaces. In the following, we will assume for simplicity that T_e is constant (but nonzero). The equilibrium equation can then be written in terms of dimensionless variables as

$$\tilde{\nabla}^2\tilde{\phi} = s(\psi)\exp(\tilde{\phi}), \tag{2}$$

where $\tilde{\phi} = e\phi/T_e$, $s(\psi) = N(\psi)/N(0)$, and the spatial dimensions are measured in units of a characteristic scale length $s_D = \sqrt{\epsilon_0 T_e/e^2 N(0)}$, which is reminiscent of the Debye length. Hence,

$$\tilde{\nabla}^2 = \frac{\partial^2}{\partial\tilde{x}^2} + \frac{\partial^2}{\partial\tilde{y}^2} + \frac{\partial^2}{\partial\tilde{z}^2},$$

where $\tilde{x} = x/s_D$, $\tilde{y} = y/s_D$, $\tilde{z} = z/s_D$. In the high temperature limit (i.e., when $a/\lambda_D \ll 1$), $s_D \approx \lambda_D$ and $N(\psi) \approx n$. In other words, the density is nearly constant on a magnetic surface. However, in the low temperature limit, i.e., $a/\lambda_D \gg 1$, $N(\psi)$ is substantially different from n and s_D is substantially different from λ_D. The variation in $s(\psi)$ is a measure of how far the plasma is from global thermal equilibrium.

The equilibrium equation, Eq. (2), can be derived from the condition that the total energy of the system be extremal against variations $\delta\tilde{\phi}$ in $\tilde{\phi}$ that are zero at the boundary of the solution domain, if the dimensionless energy is defined as[5]

$$\tilde{W}=\int (\tfrac{1}{2}(\tilde{\nabla}\tilde{\phi})^2+s(\psi)\exp\tilde{\phi})d\tilde{V} \tag{3}$$

with the integration extending over the volume of the solution domain, $d\tilde{V}=d\tilde{x}d\tilde{y}d\tilde{z}$. In order for the variational principle to hold true, one has to keep $s(\psi)$ constant when varying $\tilde{\phi}$. For perturbations satisfying this, the second order variation of $\tilde{W}$ around an equilibrium solution $\tilde{\phi}_0$ is

$$\delta\tilde{W}=\frac{1}{2}\int ((\nabla\delta\tilde{\phi})^2+(\delta\tilde{\phi})^2 s(\psi)\exp(\tilde{\phi}_0))d\tilde{V}. \tag{4}$$

Hence, the equilibrium is a minimum $\tilde{W}$ state. We cannot conclude, however, that the equilibrium is a true minimum energy state, as we have not proven that physical perturbations keep $s(\psi)$ constant, and hence, that the free energy of the system is given by $\tilde{W}$. This is a topic of current investigation. Regardless of the physical interpretation of $\tilde{W}$, the equilibrium being a minimum of $\tilde{W}$ is an interesting mathematical property of the equilibrium equation, and one that is useful for numerical solution techniques. Equivalently, one can derive the equilibrium equation from minimizing a quantity W with proper units of energy [keeping $N(\psi)$ constant],

$$W=\int (\tfrac{1}{2}\epsilon_0(\nabla\phi)^2+N(\psi)T_e(\psi)\exp(e\phi/T_e))dV. \tag{5}$$

The first term is the electrostatic energy density, whereas the second term is the pressure, nT_e.

III. NUMERICAL METHOD

A pseudospectral Fourier method has been used to solve the equilibrium equation, Eq. (2), in two dimensions, to find the equilibrium $\tilde{\phi}(x,y)$. The Laplacian decouples completely in Fourier space, which allows implicit evaluation of the Laplace term without having to solve large sets of coupled linear equations. The term pseudospectral implies that the nonlinear term, $f(\tilde{\phi})=s(\psi)\exp(\tilde{\phi})$, is evaluated in real space, i.e., $\tilde{\phi}$ is transformed from Fourier space to real space, f is calculated in real space, and then transformed to Fourier space. Denoting the Fourier coefficients by superscript $\mathbf{k}$, where $\mathbf{k}=(k_x,k_y)$ is the wave vector in Fourier space, the equilibrium equation for each Fourier mode is

$$\frac{\partial\tilde{\phi}^{\mathbf{k}}}{\partial t}=-f^{\mathbf{k}}-k^2\tilde{\phi}^{\mathbf{k}}. \tag{6}$$

Here, we have regularized the equation by adding a term $\partial\tilde{\phi}/\partial t$. This improves numerical stability. The steady state solution ($\partial\tilde{\phi}/\partial t=0$), is the equilibrium solution. The iteration formula then becomes

$$\tilde{\phi}_j^{\mathbf{k}}=\frac{\tilde{\phi}_{j-1}^{\mathbf{k}}-\delta t f_{j-1}^{\mathbf{k}}}{1+k^2\delta t}. \tag{7}$$

δt must be positive in order to achieve convergence towards the steady state solution. The boundary conditions are imposed through a method of image charges, which is described in the Appendix.

The algorithm described above was implemented in Interactive Data Language (IDL), and all the results presented here are for a spatial resolution of 128×128 grid points (and Fourier modes). In the $a/\lambda_D\ll1$ limit, $\delta t=1$ is appropriate for convergence, but in the $a/\lambda_D\gg1$ limit, convergence becomes unacceptably slow unless δt is gradually increased from one iteration to the next. In the most extreme cases ($a/\lambda_D\approx10$), δt must be increased slowly as the algorithm converges to as much as 10^{38} to ensure convergence in less than 10 000 iterations. The slow convergence can be understood as follows. In order to increase a/λ_D, we increase the size of the plasma and the domain size. For the dimensionless equilibrium equation, the scale size is s_D rather than λ_D, and the box size has to be increased from 1 to 10^{21} (in units of s_D) in order to increase the plasma radius a from $\approx0.1\lambda_D$ to $\approx10\lambda_D$. This means that k^2 in the iteration formula, Eq. (7), is smaller by 42 orders of magnitude, and δt must be increased accordingly so that $k^2\delta t$ does not become negligibly small.

Since the relation between $N(\psi)$ and n is highly nonlinear in the $a/\lambda_D\gg1$ limit, it is difficult *a priori* to guess a shape for $N(\psi)$ which produces a desired n. Therefore, for all the equilibria studied here, we have imposed a parabolic electron density profile

$$n(x,0)=1-\frac{x^2}{a^2} \tag{8}$$

on the $y=0$ line for $0\leqslant x\leqslant a$, and then calculate

$$N[\psi(x,0)]=n(x,0)e^{-\tilde{\phi}(x,0)}. \tag{9}$$

The subsequent evaluation of $N(\psi)$ for other values of ψ on the computational grid requires high accuracy interpolation of $N(\psi)$, because N varies by many orders of magnitude in the $a/\lambda_D\gg1$ limit. Because the calculation of $N(\psi)$ is computationally intensive, Eq. (7) is evaluated 100 times for each recalculation of $N(\psi)$. This does not adversely affect the convergence rate.

IV. RESULTS

The main subtlety of Eq. (1) comes from the lack of separability of ∇^2 for nontrivial $\psi(x,y,z)$, i.e., from any nontrivial shape of the magnetic surfaces. Ellipticity dominates over toroidicity as the dominant breaking of the separability as long as long as $b/a-1\gg a/R$ with a and b being the short and long ellipse axes, and R being the major radius of a generic elliptical cross section toroidal magnetic surface. In this case, a two-dimensional description may be appropriate. We focus our attention on two-dimensional equilibria with elliptic magnetic surfaces. An ellipticity $b/a=\sqrt{3}$ is used throughout the paper. The boundary conditions are those of a perfect conductor located outside the plasma. We present results from two different shapes for the perfect conductor. In each case, we investigate the $a/\lambda_D\ll1$ and the $a/\lambda_D\gg1$ limit. In each case we have confirmed numerically that the equilibrium is a minimum $\tilde{W}$ state, as defined in the previous section.

We have investigated numerically the differences between $a/\lambda_D\ll1$ (warm, thin, small) plasmas, and $a/\lambda_D\gg1$

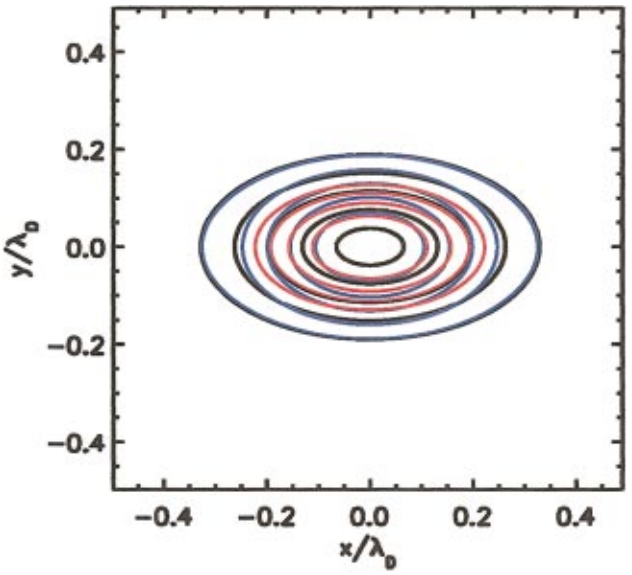

FIG. 1. (Color) Warm plasma with conforming boundary. Contours of constant $\tilde{\phi}$ (blue), n (red), and the flux surfaces (black) for a $a/\lambda_D \approx 0.1$ plasma. The outermost $\tilde{\phi}$ contour represents the perfectly conducting boundary, which matches a flux surface.

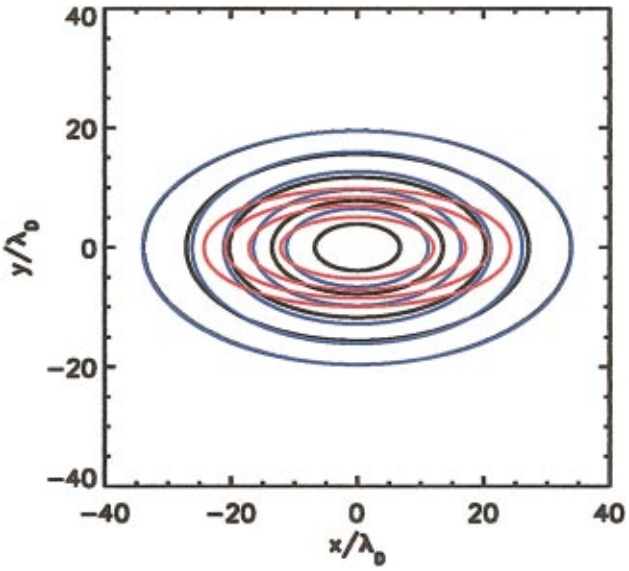

FIG. 3. (Color) Cold plasma, $a/\lambda_D \approx 10$, with conforming boundary. Contours of constant $\tilde{\phi}$ (blue), n (red), and the flux surfaces (black) for a $a/\lambda_D \approx 10$ plasma. The outermost $\tilde{\phi}$ contour represents the perfectly conducting boundary, which matches a flux surface.

(cold, dense, large) plasmas, and explored the equilibria of these plasmas for different boundary conditions. In Fig. 1 we present contours of n, $\tilde{\phi}$, and the magnetic surface coordinate ψ, for a $a/\lambda_D \approx 0.1$ plasma with a perfectly conducting boundary whose shape and location is chosen to coincide with a magnetic surface outside the edge of the plasma. It is evident that the density contours closely match the magnetic surfaces. The variation of $\tilde{\phi}$ and n on the magnetic surfaces is illustrated quantitatively by plotting $\tilde{\phi}$ and n as functions of the ψ coordinate in a scatter plot. The vertical scatter on such a plot indicates the degree to which the quantity varies on a particular magnetic surface. For the equilibrium just described, scatter plots of $\tilde{\phi}(\psi)$ and $n(\psi)$ are presented in Fig. 2. The points plotted are the values on the 128×128 grid points. Figure 2 confirms that the density is essentially constant on the magnetic surfaces, and illustrates that $\tilde{\phi}$ has some variation on the magnetic surfaces, in particular in the vacuum region and plasma edge regions. Since the boundary condition itself enforces constancy on a particular magnetic surface external to the plasma, $\tilde{\phi}$ does not vary strongly even though the plasma is relatively warm.

By increasing the plasma size from $a \approx 0.1 s_D$ to $a \approx 10^{20} s_D$, the number of Debye lengths in the plasma can be increased from $a \approx 0.1\lambda_D$ to $a \approx 10\lambda_D$. Contour plots are shown in Fig. 3. Scatter plots of $\tilde{\phi}(\psi)$ and $n(\psi)$ are shown

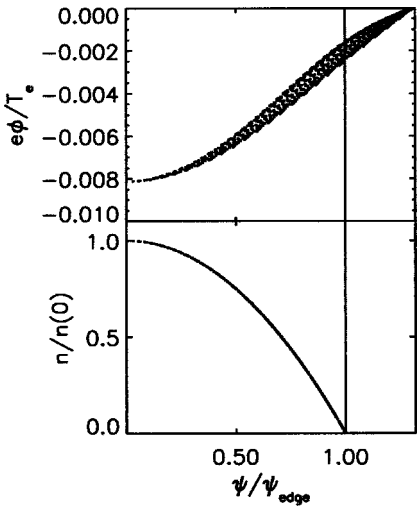

FIG. 2. Scatter plot of $\tilde{\phi}$ (top) and n (bottom) as functions of the flux surface coordinate ψ for a warm plasma, $a/\lambda_D \approx 0.1$, with perfect conductor boundary conforming to the magnetic surfaces. $\psi/\psi_a = 1$ is the edge of the plasma.

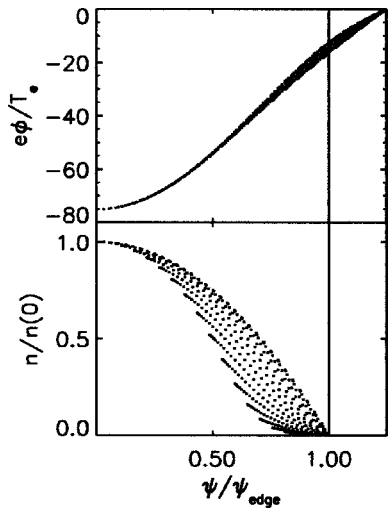

FIG. 4. Scatter plot of $\tilde{\phi}$ and n as a function of the flux surface coordinate ψ for a cold plasma with perfect conductor boundary conforming to the magnetic surfaces.

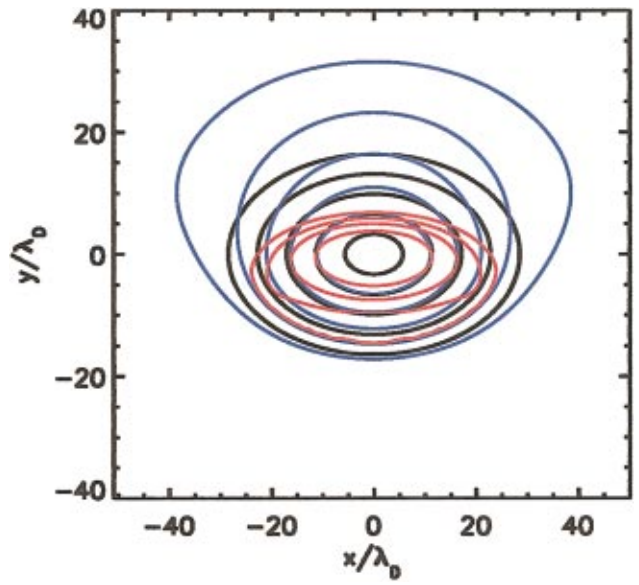

FIG. 5. (Color) Cold plasma with an asymmetric boundary. Contours of constant $\tilde{\phi}$ (blue), n (red), and the flux surfaces (black) for a $a/\lambda_D \approx 10$ plasma. The outermost $\tilde{\phi}$ contour represents the conducting boundary.

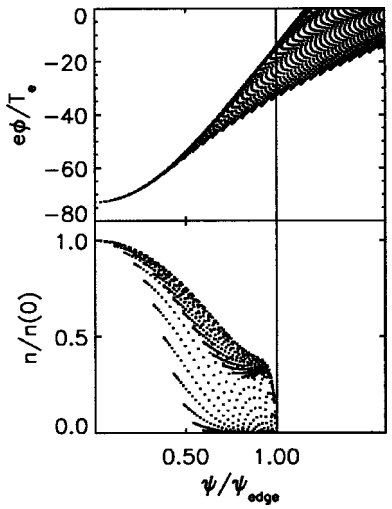

FIG. 6. Scatter plots of $\tilde{\phi}$ and n as functions of ψ for the asymmetric boundary condition shown in Fig. 5 with $a/\lambda_D \approx 10$.

in Fig. 4. The relative variation of $\tilde{\phi}$ is somewhat smaller than for the warmer plasma, and becomes very small in the plasma interior, as expected from the $T_e = 0$ equilibrium, where ϕ is constant on a magnetic surface.[1] By contrast, n varies significantly on the magnetic surfaces, in particular in the outer regions of the plasma. Numerical problems associated with the many orders of magnitude variations in $N(\psi)$ and $\exp(\tilde{\phi})$ currently limit the code to $a/\lambda_D < 10$. A modified algorithm allowing larger values of a/λ_D is currently being developed.

If indeed the true energy of the system is minimized in equilibrium, the electrostatic interaction between the image charges of the wall and the plasma will pull the plasma towards the closest part of the wall, since that will minimize the plasma energy. In Penning trap equilibria, the opposite effect was observed, the electron plasma would actually move away from positively biased conductors and towards negatively biased conductors,[6] consistent with the fact that Penning trap equilibria are maximum energy states.[6–8] By choosing a highly asymmetric perfect conductor shape, we can investigate the effect for a magnetic surface configuration, and at the same time, determine the effects of a boundary that is far from conforming with the magnetic surfaces. We choose a relatively cold plasma ($a/\lambda_D \approx 10$) such that the electrostatic energy term dominates. In the opposite limit, $a/\lambda_D \approx 0.1$, the density becomes nearly constant on the magnetic surfaces, and the electrostatic potential is mostly determined by the boundary condition rather than the plasma. Figure 5 shows the magnetic surfaces, the constant $\tilde{\phi}$ contours, and constant n contours. The outermost $\tilde{\phi}$ contour is the conducting boundary, and it is clear that the plasma is attracted towards the conductor, that is, towards the positive image charges on the conductor surface, as expected for a minimum energy state, and in contradiction with what would be observed for a maximum energy state. This illustrates that the equilibrium of a pure electron plasma confined on magnetic surfaces is fundamentally different from previously studied configurations. This is not an effect of toroidicity, but is an effect of the magnetic surfaces themselves; a pure toroidal field configuration (which is a closed field line system without magnetic surfaces) has a maximum energy equilibrium state.[9]

Figure 6 shows that the electrostatic potential becomes nearly constant on the magnetic surfaces in the plasma interior even in this asymmetric case, and that the density varies strongly on magnetic surfaces. There is significant variation of the electrostatic potential near the plasma edge despite the fact that this is a small Debye length plasma. Note that the large variations in $\tilde{\phi}$ occur on magnetic surfaces where the density drops to near zero on at least part of the surface. On the density depleted part of the surface, the electron plasma cannot shield out the externally imposed variations in $\tilde{\phi}$.

V. DISCUSSION

Regardless of the particular shape of conducting structures surrounding the plasma, experimentally relevant equilibria exist, i.e., equilibria where the density goes smoothly to zero at the plasma edge. In the large Debye length limit, $a/\lambda_D \ll 1$, the pressure gradient term dominates over the electric field term, and plasma pressure becomes nearly constant on magnetic surfaces, as must the density, since the temperature is assumed constant on the surfaces due to rapid parallel heat conduction. In this limit, $\tilde{\phi}$ is strongly influenced by the boundary conditions and may vary significantly on magnetic surfaces, even in the plasma interior, unless the boundary conditions are chosen carefully.

In the opposite limit, $a/\lambda_D \gg 1$, the electric field term dominates over the pressure gradient term. In this case, $\tilde{\phi}$ becomes nearly constant on magnetic surfaces, except in the vacuum and plasma edge regions, where the boundary conditions are important and may impose some variation of $\tilde{\phi}$ on a magnetic surface. However, the relative variation of n

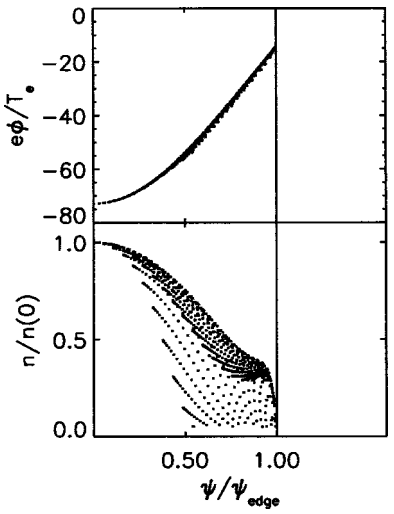

FIG. 7. Scatter plots of $\tilde{\phi}$ and n as functions of ψ, excluding points where n is less than 5% of the central density, for the same equilibrium shown in Figs. 5 and 6.

on a magnetic surface is exponentially related to the absolute variation of $\tilde{\phi}$ on the surface. This follows immediately from $n=N(\psi)e^{\tilde{\phi}}$. Thus, as the plasma approaches the $a/\lambda_D \gg 1$ limit, the $\tilde{\phi}=$const surfaces conform increasingly to the $\psi=$const surfaces (the magnetic surfaces) but the absolute variation of $\tilde{\phi}$ on the outer magnetic surfaces is nonetheless observed to increase.

The collisional confinement time depends on the degree to which the magnetic surfaces match the surfaces of constant $\tilde{\phi}$.[1] The numerical results presented here indicate that the neoclassical transport will generally be larger at the edge of the plasma than at the center, will be significantly affected by the boundary conditions, and can be reduced by choosing a perfect conductor with an appropriate shape, e.g., conforming to the magnetic surfaces. However, the largest variations in $\tilde{\phi}$ occur on the part of a magnetic surface where the density is depleted, and hence, only an exponentially small fraction of the plasma particles actually reside in the regions of relatively poor confinement. We illustrate this in Fig. 7, which is a replot of Fig. 6 except that all points with a density less than 5% of the central density have been excluded. It is evident that $\tilde{\phi}$ is nearly constant on magnetic surfaces in regions where there is appreciable plasma density, despite the highly asymmetric boundary condition. This effect, which will become even more pronounced at higher values of a/λ_D, acts to significantly reduce the transport rate across the magnetic surfaces.

ACKNOWLEDGMENTS

The author would like to thank Professor Guillaume Bal for important advice on the numerical algorithm and Professor Allen H. Boozer for valuable discussions regarding the equilibrium equation.

APPENDIX: NUMERICAL IMPLEMENTATION OF BOUNDARY CONDITIONS

A simple Fourier spectral method, such as the one used here, automatically enforces periodic boundary conditions. This is not a very serious constraint since the box size can be made large enough that the periodicity does not constrain the possible solutions in the interior of the box. However, the periodicity in ϕ automatically enforces that the average value of $\nabla^2\phi$ [i.e., the (0,0) Fourier mode] must be zero, that is, the net charge in the computational box must be zero. For example, if a perfect conductor boundary condition is imposed, the total positive surface charge on the conductor will add up to the total negative charge in the pure electron plasma. Such a surface charge corresponds to a Dirac's δ function in charge density on the conductor. There will inevitably be severe ''ringing,'' effects if one tries to impose such a sharp boundary condition when using a simple Fourier spectral method. Therefore, a different, indirect way of imposing different boundary conditions was used. A smooth distribution of positive charges is placed well outside the plasma region, such that there is a vacuum region separating the negative charges of the plasma and the surrounding positive charges. Numerically, this is done by adding the positive space charge contribution to the right hand side of the equilibrium equation, Eq. (2),

$$f(x,y)=s(\psi)\exp(\tilde{\phi}(x,y))-P(x,y). \tag{A1}$$

At each time step, the positive charge distribution is scaled up or down by a scalar factor so that the net charge remains zero.

By varying the shape and location of the positive charge distribution, the shape of $\phi=$const surfaces can be changed, and can be made arbitrarily close to, e.g., an elliptical magnetic surface, somewhere in the vacuum region between the negative and positive charges. The solution inside of the elliptical $\phi=$const surface is identical to that which would be obtained by placing a perfect conductor there. The simple conductor shapes investigated here can be imposed by manually changing the shape of the external positive charge distribution until the desired shape (e.g., conforming to a magnetic surface), is obtained. The method is not practical for arbitrarily shaped perfect conductors.

A constant can always be added to ϕ without changing the physical solution, as long as $N(\psi)$ is scaled accordingly. In the scatter plots presented in this paper, an extra constant has been added to the numerical solutions for $\tilde{\phi}$, such that $\tilde{\phi}=0$ on the perfectly conducting boundary.

[1] T. S. Pedersen and A. H. Boozer, Phys. Rev. Lett. **88**, 205002 (2002).
[2] Z. Yoshida, Y. Ogawa, J. Morikawa *et al.*, AIP Conf. Proc. **498**, 397 (1999).
[3] J. S. deGrassie and J. H. Malmberg, Phys. Rev. Lett. **39**, 1077 (1977).
[4] L. Brillouin, Phys. Rev. **67**, 260 (1945).
[5] A. H. Boozer (private communication, 2002).
[6] J. Notte, A. J. Peurrung, J. Fajans, R. Chu, and J. S. Wurtele, Phys. Rev. Lett. **69**, 3056 (1992).
[7] T. M. O'Neil and R. A. Smith, Phys. Fluids B **4**, 2720 (1992).
[8] R. Chu, J. Wurtele, J. Notte, A. J. Peurrung, and J. Fajans, Phys. Fluids B **5**, 2378 (1993).
[9] T. O'Neil and R. Smith, Phys. Plasmas **1**, 2430 (1994).